

Supporting Information for

Preparation of Thermochromic Selenidostannates in Deep Eutectic Solvents

Kai-Yao Wang,^a Dong Ding,^a Shu Zhang,^a Yanlong Wang,^b Wei Liu,^b Shuao Wang,^b Shuai-Hua Wang,^c Dan Liu^a and Cheng Wang*^a

^a *Institute for New Energy Materials and Low-Carbon Technologies, School of Materials Science and Engineering, Tianjin University of Technology, Tianjin 300384, P. R. China, E-mail: cawang@tjut.edu.cn.*

^b *School for Radiological and Interdisciplinary Sciences (RAD-X), Soochow University; Collaborative Innovation Center of Radiation Medicine of Jiangsu Higher Education Institutions, Suzhou 215123, P. R. China.*

^c *Fujian Institute of Research on the Structure of Matter, Chinese Academy of Sciences, Fuzhou 350108, P. R. China*

1. Materials and Methods

All reagents and chemicals were purchased from commercial sources and were used without further purification. FTIR spectra (KBr pellets) were recorded on a PerkinElmer Frontier Mid-IR FTIR spectrometer. Raman spectra were recorded on a Horiba Evolution Raman spectrometer with a 532 nm green laser in the range of 50-800 cm⁻¹. The beam was focused on the sample through a confocal microscope using a × 100 objective lens. Temperature-dependent single-crystal UV/Vis absorption spectra were recorded on a Craic Technologies microspectrophotometer. Crystals were placed on quartz slides under Krytox oil, and data was collected after optimization of microspectrophotometer. Temperature-dependent reflectance spectra of the smooth polycrystalline sample were collected on an Ideaoptics PG2000L spectrometer equipped with a HL2000 tungsten halogen light source (color temperature: 2915 K) and a FIB-Y-600-DUV fiber reflection probe placed at a 45° orientation, and the STD-WS was used as the diffuse reflection standard (100% reflectance). The resulting color coordinates (*x*, *y*, *z*) values were calculated by the Morpho 3.2 software using D65 light source (color temperature: 6500 K) as the standard illuminant. Thermogravimetric analysis were performed on a Netzsch TG 209 F3 device at a heating rate of 10 °C min⁻¹ under nitrogen. ¹H and ¹³C NMR spectra of the compounds dissolved in N₂H₄·H₂O/D₂O were recorded on a Bruker Avance III 400 instrument at room temperature by using 5 mm tubes. The respective resonance frequencies were 400.53 MHz (¹H) and 100.71 MHz (¹³C), and the chemical shifts are reported with respect to the references Si(CH₃)₄. Room temperature powder X-ray diffraction (XRD) patterns were collected in the angular range of 2θ = 5-80° on a Rigaku SmartLab 9KW diffractometer

using Cu- $K\alpha$ radiation. Temperature-dependent powder XRD patterns were recorded on the Rigaku XtaLab PRO single-crystal X-ray diffractometer using the powder power tool (Cu- $K\alpha$ radiation). Elemental analysis on H, C and N were performed on an Elementar Vario EL cube instrument.

2. Synthesis

Synthesis of $[(\text{CH}_3)_3\text{N}(\text{CH}_2)_2\text{OH}]_2[\text{Sn}_3\text{Se}_7]\cdot\text{H}_2\text{O}$ (1): A mixture of Sn (0.119 g, 1.0 mmol), Se (0.211 g, 2.67 mmol), choline chloride (1.12 g, 8.0 mmol), urea (0.96 g, 16.0 mmol) and 1.0 mL $\text{N}_2\text{H}_4\cdot\text{H}_2\text{O}$ (98%) (~20.6 mmol) was sealed in a stainless steel reactor with 20 mL Teflon liner, and heated at 150 °C for 24 hours. After cooling to room temperature by natural ventilation, the product was washed with distilled water and then dried in the air. Plate-like orange crystals of **1** were collected in a yield of 0.257 g, 68% based on Sn. Anal. Calc. for $\text{C}_{10}\text{H}_{30}\text{N}_2\text{O}_3\text{Se}_7\text{Sn}_3$ (**1**): C, 10.58%; H, 2.66%; N, 2.47%; found: C, 10.54%; H, 2.67%; N, 2.87%.

Synthesis of $[(\text{CH}_3)_3\text{N}(\text{CH}_2)_2\text{CH}_3]_2[\text{Sn}_3\text{Se}_7]$ (2): A mixture of Sn (0.119 g, 1.0 mmol), Se (0.211 g, 2.67 mmol), trimethylpropylammonium bromide (1.456 g, 8.0 mmol), urea (0.96 g, 16.0 mmol) and 1.0 mL $\text{N}_2\text{H}_4\cdot\text{H}_2\text{O}$ (98%) (~20.6 mmol) was sealed in a stainless steel reactor with 20 mL Teflon liner, and heated at 150 °C for 24 hours. After cooling to room temperature by natural ventilation, the product was washed with distilled water and then dried in the air. Plate-like orange crystals of **2** were collected in a yield of 0.216 g, 58% based on Sn. Anal. Calc. for $\text{C}_{12}\text{H}_{32}\text{N}_2\text{Se}_7\text{Sn}_3$ (**2**): C, 12.95%; H, 2.90%; N, 2.52%; found: C, 12.41%; H, 3.04%; N, 2.59%.

3. Crystallography

Single crystals of **1-100K** ~ **1-290K** and **2-100K** ~ **2-470K** were mounted on a Hampton cryo-loop for data collection. Indexing and data collection were performed on a with a Rigaku XtaLab PRO diffractometer with graphite monochromated Mo- $K\alpha$ radiation ($\lambda = 0.71073 \text{ \AA}$) in the temperature range of 100 K to 470 K. The absorption corrections were applied using a multi-scan technique. Direct methods (SHELXS97) successfully located the tin and selenium atoms, and successive Fourier syntheses (SHELXL2014) revealed the remaining atoms.^[1] Refinements were conducted by full-matrix least squares against $|F|^2$ using all data. Non-hydrogen atoms were refined with anisotropic displacement parameters and the hydrogen atoms bonded to C, N and O atoms were positioned with idealized geometry. The relevant crystallographic data and structure-refinement details are shown in Table S1-S4. CCDC for **1**: 1821848 (100 K), 1836567 (130 K), 1836568 (170 K), 1836565 (210 K), 1836564 (250 K), 1836566 (290 K); for **2**: 1821847 (100 K), 1836570 (130 K), 1836572 (170 K), 1836571 (210 K), 1836569 (250 K), 1836574 (290 K), 1836577 (320 K), 1836576 (370 K), 1836575 (420 K), 1836573 (470 K). These data can be obtained free of charge from The Cambridge Crystallographic Data Centre.

4. Tables

Table S1. Crystal data for **1-100K**, **1-130K** and **1-170K**.

Compound	1-100K	1-130K	1-170K
Empirical formula	C ₁₀ H ₃₀ N ₂ O ₃ Se ₇ Sn ₃	C ₁₀ H ₃₀ N ₂ O ₃ Se ₇ Sn ₃	C ₁₀ H ₃₀ N ₂ O ₃ Se ₇ Sn ₃
Formula weight	1135.15	1135.15	1135.15
Crystal system	monoclinic	monoclinic	monoclinic
Space group	<i>P2₁/n</i>	<i>P2₁/n</i>	<i>P2₁/n</i>
T/K	100(2)	130(2)	170(2)
$\lambda/\text{\AA}$	0.71073	0.71073	0.71073
<i>a</i> /\AA	9.8365(3)	9.8469(3)	9.8761(3)
<i>b</i> /\AA	13.5796(4)	13.5734(5)	13.5970(5)
<i>c</i> /\AA	20.7384(7)	20.7529(7)	20.7839(6)
α°	90	90	90
β°	92.727(3)	92.642(3)	92.484(3)
γ°	90	90	90
<i>V</i> /\AA ³	2767.01(15)	2770.80(16)	2788.35(16)
<i>Z</i>	4	4	4
<i>D_c</i> /Mg·m ⁻³	2.725	2.721	2.704
μ/mm^{-1}	11.908	11.891	11.816
<i>F</i> (000)	2064	2064	2064
Measured refls.	27310	27103	28291
Independent refls.	5601	5609	5636
<i>R</i> _{int}	0.0680	0.0599	0.0587
No. of parameters	210	210	210
<i>GOF</i>	1.010	1.004	1.005
<i>R</i> ₁ , ^[a] <i>wR</i> ₂ [<i>I</i> > 2σ(<i>I</i>)]	0.0424, 0.0922	0.0472, 0.1089	0.0415, 0.0946
<i>R</i> ₁ , <i>wR</i> ₂ (all data)	0.0551, 0.0974	0.0592, 0.1151	0.0533, 0.1000
CCDC	1821848	1836567	1836568

^[a] $R_1 = \sum ||F_o| - |F_c|| / \sum |F_o|$, $wR_2 = \{ \sum w[(F_o)^2 - (F_c)^2]^2 / \sum w[(F_o)^2]^2 \}^{1/2}$

Table S2. Crystal data for **1-210K**, **1-250K**, and **1-290K**.

Compound	1-210K	1-250K	1-290K
Empirical formula	C ₁₀ H ₃₀ N ₂ O ₃ Se ₇ Sn ₃	C ₁₀ H ₃₀ N ₂ O ₃ Se ₇ Sn ₃	C ₁₀ H ₃₀ N ₂ O ₃ Se ₇ Sn ₃
Formula weight	1135.15	1135.15	1135.15
Crystal system	monoclinic	monoclinic	monoclinic
Space group	<i>P2₁/n</i>	<i>P2₁/n</i>	<i>P2₁/n</i>
T/K	210(2)	250(2)	290(2)
$\lambda/\text{\AA}$	0.71073	0.71073	0.71073
<i>a</i> /\AA	9.8956(4)	9.9152(4)	9.9739(5)
<i>b</i> /\AA	13.6110(5)	13.6371(5)	13.7151(6)
<i>c</i> /\AA	20.8327(7)	20.9056(8)	21.1612(9)
$\alpha/^\circ$	90	90	90
$\beta/^\circ$	92.368(3)	92.274(4)	91.969(4)
$\gamma/^\circ$	90	90	90
<i>V</i> /\AA ³	2803.54(18)	2824.52(19)	2893.0(2)
<i>Z</i>	4	4	4
<i>D_c</i> /Mg·m ⁻³	2.689	2.669	2.606
μ/mm^{-1}	11.752	11.665	11.389
<i>F</i> (000)	2064	2064	2064
Measured refls.	26407	26733	26559
Independent refls.	5678	5725	5885
<i>R</i> _{int}	0.0638	0.0631	0.0682
No. of parameters	210	210	174
<i>GOF</i>	1.005	1.004	1.005
<i>R</i> ₁ , ^[a] <i>wR</i> ₂ [<i>I</i> > 2 σ (<i>I</i>)]	0.0417, 0.0973	0.0389, 0.0883	0.0440, 0.1029
<i>R</i> ₁ , <i>wR</i> ₂ (all data)	0.0555, 0.1036	0.0531, 0.0946	0.0641, 0.1129
CCDC	1836565	1836564	1836566

^[a] $R_1 = \sum ||F_o| - |F_c|| / \sum |F_o|$, $wR_2 = \{\sum w[(F_o)^2 - (F_c)^2]^2 / \sum w[(F_o)^2]^2\}^{1/2}$

Table S3. Crystal data for **2-100K**, **2-130K**, **2-170K**, **2-210K** and **2-250K**.

Compound	2-100K	2-130K	2-170K	2-210K	2-250K
Empirical formula	C ₁₂ H ₃₂ N ₂ Se ₇ Sn ₃	C ₁₂ H ₃₂ N ₂ Se ₇ Sn ₃	C ₁₂ H ₃₂ N ₂ Se ₇ Sn ₃	C ₁₂ H ₃₂ N ₂ Se ₇ Sn ₃	C ₁₂ H ₃₂ N ₂ Se ₇ Sn ₃
Formula weight	1113.18	1113.18	1113.18	1113.18	1113.18
Crystal system	orthorhombic	orthorhombic	orthorhombic	orthorhombic	orthorhombic
Space group	<i>Pbca</i>	<i>Pbca</i>	<i>Pbca</i>	<i>Pbca</i>	<i>Pbca</i>
T/K	100(2)	130(2)	170(2)	210(2)	250(2)
λ / Å	0.71073	0.71073	0.71073	0.71073	0.71073
<i>a</i> / Å	17.4028(11)	17.4184(15)	17.4508(12)	17.5861(12)	17.4944(14)
<i>b</i> / Å	13.7025(6)	13.6963(6)	13.6959(8)	13.7084(7)	13.7191(8)
<i>c</i> / Å	23.9113(9)	23.9378(14)	23.9469(17)	23.9914(12)	24.0762(12)
α /°	90	90	90	90	90
β /°	90	90	90	90	90
γ /°	90	90	90	90	90
<i>V</i> / Å ³	5701.9(5)	5710.8(7)	5723.4(7)	5783.8(6)	5778.5(6)
<i>Z</i>	8	8	8	8	8
<i>D_c</i> / Mg·m ⁻³	2.593	2.589	2.584	2.557	2.559
μ /mm ⁻¹	11.547	11.529	11.503	11.383	11.394
<i>F</i> (000)	4048	4048	4048	4048	4048
Measured refls.	56029	49440	49714	50716	44455
Independent refls.	5818	6299	6310	7703	6369
<i>R</i> _{int}	0.1132	0.1252	0.1528	0.1235	0.1432
No. of parameters	191	191	191	190	157
<i>GOF</i>	1.031	1.020	1.042	1.059	1.031
<i>R</i> ₁ , ^[a] <i>wR</i> ₂ [<i>I</i> > 2 σ (<i>I</i>)]	0.0775, 0.1756	0.0888, 0.1956	0.1121, 0.2386	0.0886, 0.1756	0.0812, 0.1766
<i>R</i> ₁ , <i>wR</i> ₂ (all data)	0.1097, 0.1958	0.1305, 0.2185	0.1547, 0.2625	0.1531, 0.2030	0.1336, 0.2043
CCDC	1821847	1836570	1836572	1836571	1836569

^[a] $R_1 = \sum ||F_o| - |F_c|| / \sum |F_o|$, $wR_2 = \{ \sum w[(F_o)^2 - (F_c)^2]^2 / \sum w[(F_o)^2]^2 \}^{1/2}$

Table S4. Crystal data for **2-290K**, **2-320K**, **2-370K**, **2-420K** and **2-470K**.

Compound	2-290K	2-320K	2-370K	2-420K	2-470K
Empirical formula	C ₁₂ H ₃₂ N ₂ Se ₇ Sn ₃	C ₁₂ H ₃₂ N ₂ Se ₇ Sn ₃	C ₁₂ H ₃₂ N ₂ Se ₇ Sn ₃	C ₁₂ H ₃₂ N ₂ Se ₇ Sn ₃	C ₁₂ H ₃₂ N ₂ Se ₇ Sn ₃
Formula weight	1113.18	1113.18	1113.18	1113.18	1113.18
Crystal system	orthorhombic	orthorhombic	orthorhombic	orthorhombic	orthorhombic
Space group	<i>Pbca</i>	<i>Pbca</i>	<i>Pbca</i>	<i>Pbca</i>	<i>Pbca</i>
T/K	290(2)	320(2)	370(2)	420(2)	470(2)
λ / Å	0.71073	0.71073	0.71073	0.71073	0.71073
<i>a</i> / Å	17.5344(14)	17.5771(13)	17.645(2)	17.7039(13)	17.7542(12)
<i>b</i> / Å	13.7273(9)	13.7282(8)	13.7539(9)	13.7664(8)	13.8310(8)
<i>c</i> / Å	24.1221(13)	24.1464(13)	24.1705(16)	24.2192(12)	24.2599(12)
α /°	90	90	90	90	90
β /°	90	90	90	90	90
γ /°	90	90	90	90	90
<i>V</i> / Å ³	5806.2(7)	5826.6(6)	5866.0(9)	5902.7(6)	5957.2(6)
<i>Z</i>	8	8	8	8	8
<i>D_c</i> / Mg·m ⁻³	2.547	2.538	2.521	2.505	2.482
μ /mm ⁻¹	11.339	11.300	11.224	11.154	11.052
<i>F</i> (000)	4048	4048	4048	4048	4048
Measured refls.	48267	49302	46295	27521	33674
Independent refls.	5919	6423	6475	6017	6566
<i>R</i> _{int}	0.1176	0.1209	0.1348	0.0951	0.1130
No. of parameters	155	155	149	149	148
<i>GOF</i>	1.021	1.095	1.069	1.027	1.038
<i>R</i> ₁ , ^[a] <i>wR</i> ₂ [<i>I</i> > 2σ(<i>I</i>)]	0.0701, 0.1576	0.0734, 0.1690	0.0826, 0.1735	0.0762, 0.1687	0.0929, 0.2012
<i>R</i> ₁ , <i>wR</i> ₂ (all data)	0.1076, 0.1821	0.1215, 0.1924	0.1411, 0.2010	0.1545, 0.2016	0.1925, 0.2432
CCDC	1836574	1836577	1836576	1836575	1836573

^[a] $R_1 = \sum ||F_o| - |F_c|| / \sum |F_o|$, $wR_2 = \{ \sum w[(F_o)^2 - (F_c)^2]^2 / \sum w[(F_o)^2]^2 \}^{1/2}$

Table S5. Selected hydrogen-bonding data for **1-100K** and **2-100K**^a.

D-H···A	d(D-H)	d(H···A)	d(D···A)	<(DHA)
[(CH₃)₃N(CH₂)₂OH]₂[Sn₃Se₇]·H₂O (1-100K)				
O(1)-H(1D)···Se(2)#4	0.84	2.64	3.368(10)	145.6
O(2)-H(2D)···O(1W)	0.84	2.34	2.91(4)	125.0
C(2)-H(2B)···Se(7)	0.98	3.09	3.983(15)	152.1
C(2)-H(2C)···O(1)	0.98	2.32	2.989(19)	125.1
C(3)-H(3B)···Se(5)#5	0.98	3.15	3.656(12)	113.6
C(3)-H(3C)···Se(2)#6	0.98	2.92	3.854(13)	160.4
C(4)-H(4B)···Se(6)#2	0.99	3.12	3.787(13)	125.7
C(4)-H(4B)···Se(7)	0.99	2.99	3.904(12)	153.3
C(6)-H(6A)···O(2)	0.98	2.01	2.75(4)	130.0
C(6)-H(6B)···Se(6)	0.98	3.13	4.03(2)	153.4
C(6)-H(6C)···Se(3)#2	0.98	3.10	3.94(2)	145.7
C(7)-H(7A)···Se(6)	0.98	3.03	3.951(18)	158.0
C(7)-H(7B)···Se(1)#7	0.98	3.11	4.022(19)	156.3
C(8)-H(8C)···Se(6)#8	0.98	2.92	3.549(14)	123.2
C(10)-H(10B)···Se(5)#7	0.99	3.18	3.91(4)	131.4
O(1W)-H(1WA)···Se(5)#9	0.85	2.85	3.64(3)	156.2
[(CH₃)₃N(CH₂)₂CH₃]₂[Sn₃Se₇] (2-100K)				
C(1)-H(1A)···Se(2)#4	0.98	2.96	3.82(4)	147.1
C(1)-H(1C)···Se(7)	0.98	3.14	4.08(4)	160.6
C(2)-H(2C)···Se(6)#2	0.98	3.10	4.00(3)	153.3
C(9)-H(9C)···Se(4)	0.98	3.07	4.01(4)	163.5
C(4)-H(4A)···Se(1)#4	0.99	3.14	3.97(5)	141.8
C(3)-H(3A)···Se(3)#4	0.98	2.90	3.83(5)	158.0
C(3)-H(3B)···Se(5)	0.98	3.06	3.81(5)	134.2
C(3)-H(3C)···Se(6)#2	0.98	3.00	3.88(5)	150.7
C(8)-H(8A)···Se(5)#5	0.98	2.82	3.61(3)	138.7
C(8)-H(8C)···Se(3)#2	0.98	3.13	3.89(4)	135.9
C(7)-H(7A)···Se(7)#5	0.98	3.11	3.96(6)	146.6
C(7)-H(7B)···Se(5)	0.98	3.13	3.64(5)	113.7
C(7)-H(7B)···Se(6)#2	0.98	2.99	3.95(6)	168.3
C(7)-H(7C)···Se(4)	0.98	3.06	3.98(4)	157.5
C(5)-H(5A)···Se(1)#4	0.99	3.08	3.96(7)	148.8

^aSymmetry transformations used to generate equivalent atoms:

For **1-100K**: #2 $-x+3/2, y+1/2, -z+1/2$; #4 $-x+5/2, y+1/2, -z+1/2$; #5 $-x+2, -y+1, -z+1$; #6 $x-1/2, -y+3/2, z+1/2$; #7 $x-1, y, z$; #8 $-x+1/2, y+1/2, -z+1/2$; #9 $-x+1, -y+1, -z+1$.

For **2-100K**: #1 $-x, -y, -z+1$; #2 $-x, y-1/2, -z+1/2$; #4 $x+1/2, y, -z+1/2$; #5 $-x+1/2, y-1/2, z$.

Table S6. Summary of the band gaps of $[\text{Sn}_3\text{Se}_7]_n^{2n-}$ layer-containing compounds in the literature.

Compound	Space group	Band gap	Ref.
$\text{Cs}_2\text{Sn}_3\text{Se}_7$	$C2/c$	NA	[2]
$[\text{enH}_2][\text{Sn}_3\text{Se}_7] \cdot 0.5\text{en}$	$Fdd2$	NA	[3]
$(\text{TMA})_2\text{Sn}_3\text{Se}_7$	$P2_12_12_1$	2.12 eV	[4]
$(\text{C}_7\text{N}_4\text{OH}_{16})_2\text{Sn}_3\text{Se}_7 \cdot \text{H}_2$	$Pbca$	NA	[5]
$[(\text{C}_2\text{H}_5)_3\text{NH}]_2\text{Sn}_3\text{Se}_7 \cdot 0.25\text{H}_2\text{O}$	$P2_1/n$	2.1 eV	[6]
$(\text{NH}_3(\text{CH}_2)_8\text{NH}_3)\text{Sn}_3\text{Se}_7$	$P\bar{1}$	NA	[7]
$(\text{NH}_3(\text{CH}_2)_{10}\text{NH}_3)\text{Sn}_3\text{Se}_7$	$C2/c$	NA	[7]
$[\text{Mn}(\text{peha})][\text{Sn}_3\text{Se}_7]$	$P2_1/n$	NA	[8]
$[\text{Fe}(\text{phen})_3]_n(\text{Sn}_3\text{Se}_7)_n \cdot 1.25n\text{H}_2\text{O}$	$R\bar{3}c$	1.97 eV	[9]
$[\text{prmmim}]_2[\text{Sn}_3\text{Se}_7]$	$P322_1$	NA	[10]
$[\text{bmmim}]_2[\text{Sn}_3\text{Se}_7]$	$P322_1$	2.2 eV	[10]
$[\text{DBNH}]_2[\text{Sn}_3\text{Se}_7] \cdot \text{PEG}$	$C2/c$	2.13 eV	[11]
$[\text{DBNH}]_3[\text{NH}_4][\text{Sn}_6\text{Se}_{14}]$	$R\bar{3}$	2.02 eV	[11]
$[\text{Mn}(\text{dien})_2]\text{Sn}_3\text{Se}_7 \cdot 0.5\text{H}_2\text{O}$	$P2_1/n$	1.89 eV	[12]
$[\text{Fe}(\text{tatda})]\text{Sn}_3\text{Se}_7$	$P2_1/n$	1.93 eV	[12]
$[\text{Mn}(\text{en})_{2.5}(\text{en-Me})_{0.5}][\text{Sn}_3\text{Se}_7]$	$P2_1/c$	NA	[13]
$[\text{Mn}(\text{en})_3]\text{Sn}_3\text{Se}_7$	$P2_1/n$	1.99 eV	[14]
$[\text{Mn}(\text{dien})_2]\text{Sn}_3\text{Se}_7 \cdot \text{H}_2\text{O}$	$P2_1/n$	2.04 eV	[14]
$(\text{H}^+\text{-DBN})_2[\text{Sn}_3\text{Se}_7]$	$Cmc2_1$	2.02 eV	[15]

5. Figures

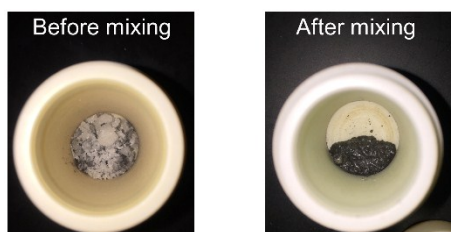


Figure S1. Photographs of the reactants, i.e. Sn, Se, ChCl, urea (without $\text{N}_2\text{H}_4 \cdot \text{H}_2\text{O}$), before and after being mixed. The transforming from bulk solid reactants to a viscous liquid mixture after being stirred indicates the formation of ChCl-urea DES.

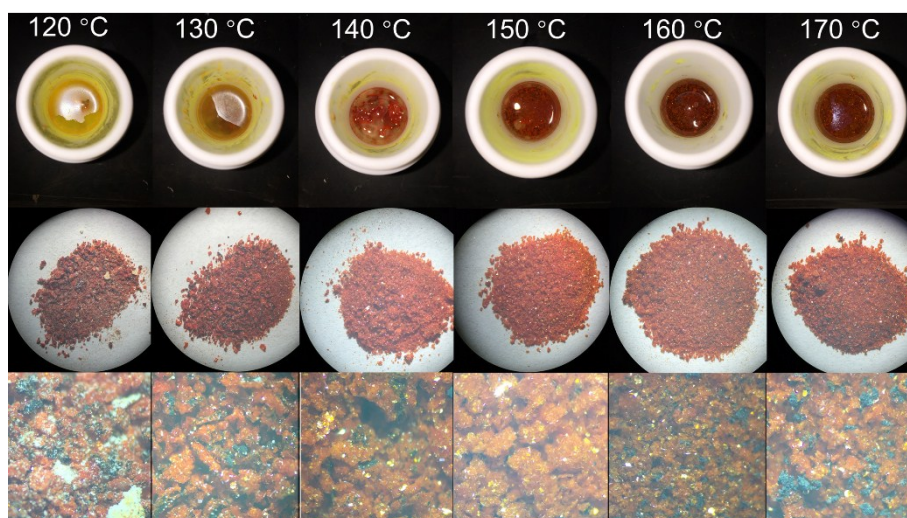


Figure S2. Photographs of the products obtained from the reactions (Sn, Se, ChCl, urea, $\text{N}_2\text{H}_4 \cdot \text{H}_2\text{O}$) performed at different temperatures. Top line: untreated products in Teflon liners; middle line: products washed by distilled water; bottom line: magnified imaging of the middle line products.

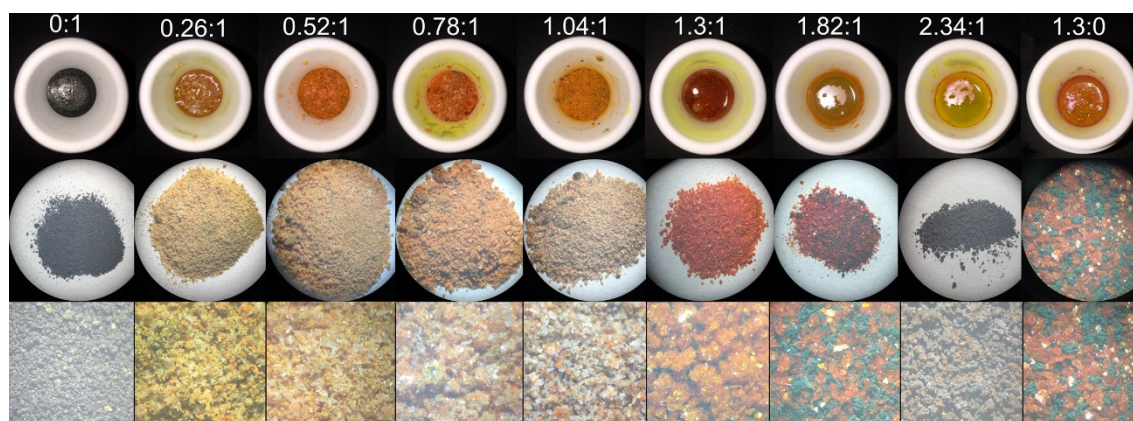


Figure S3. Photographs of the products obtained from the reactions with different $\text{N}_2\text{H}_4 \cdot \text{H}_2\text{O}$:urea molar ratios at 150 °C. Top line: untreated products in Teflon liners; middle line: products washed by distilled water; bottom line: magnified imaging of the middle line products.

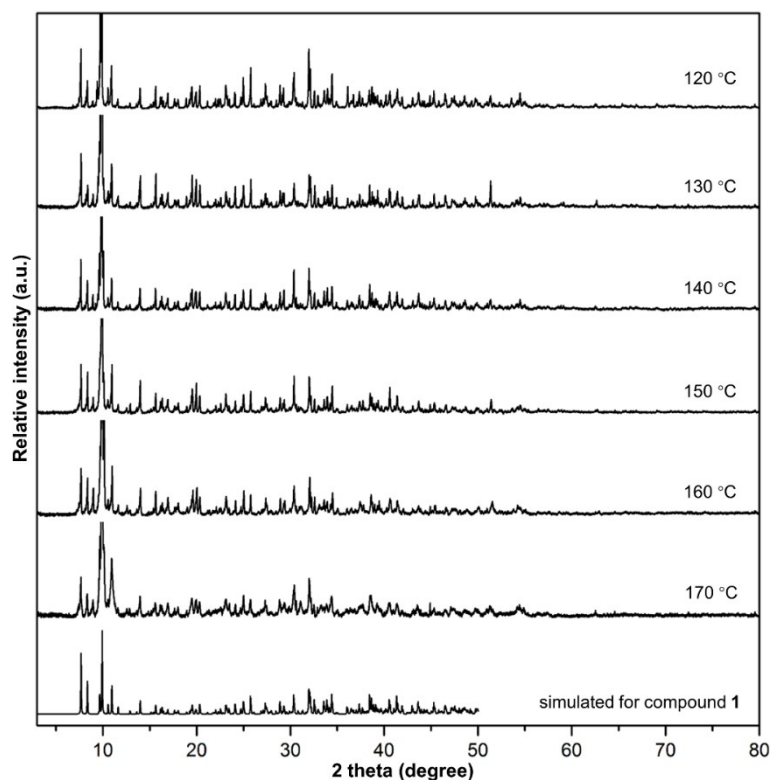


Figure S4. PXR D patterns for the products obtained from the reactions performed at 120-170 °C. The molar ratio of $\text{N}_2\text{H}_4 \cdot \text{H}_2\text{O}:\text{urea}$ for all the reactions is 1.3:1.

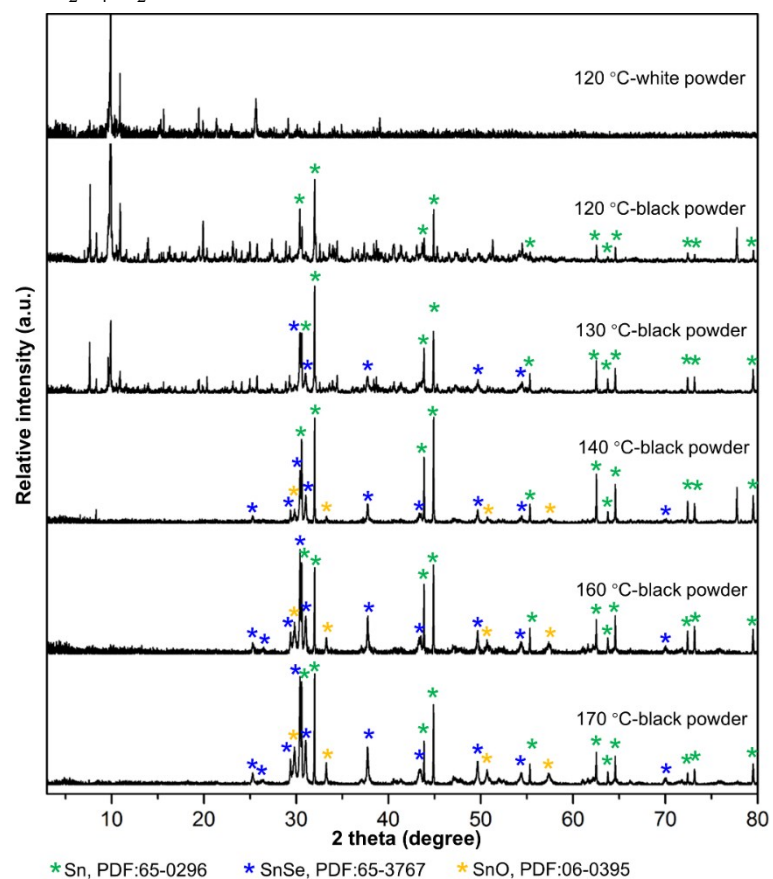


Figure S5. PXR D patterns for the by-products obtained from the reactions performed at 120-170 °C. The molar ratio of $\text{N}_2\text{H}_4 \cdot \text{H}_2\text{O}:\text{urea}$ for all the reactions is 1.3:1.

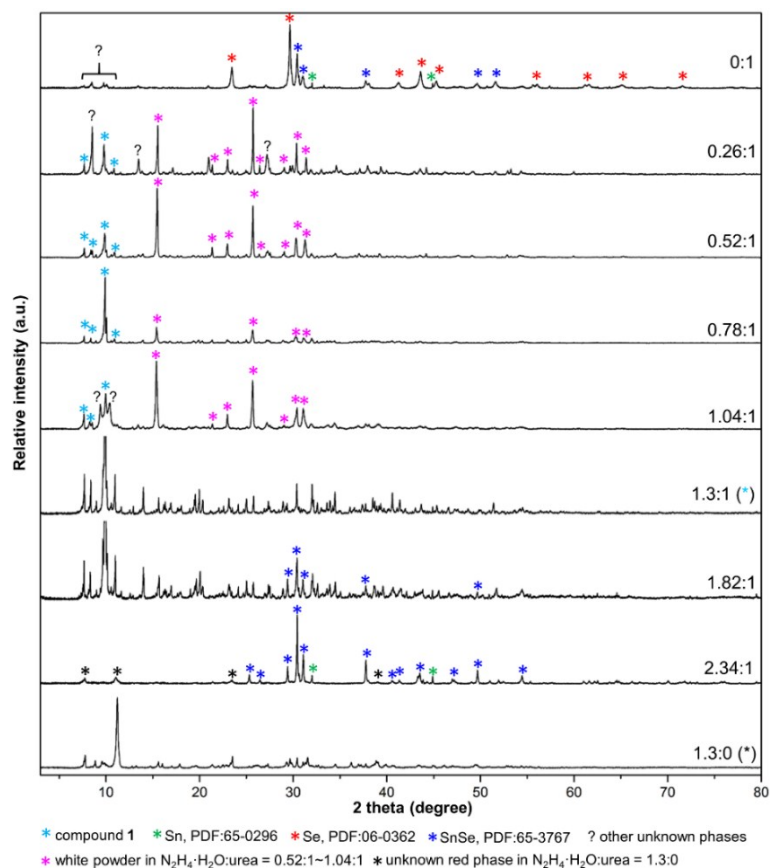


Figure S6. PXRD patterns for the products obtained from the reactions with different $\text{N}_2\text{H}_4\cdot\text{H}_2\text{O}:\text{urea}$ ratio at 150 °C.

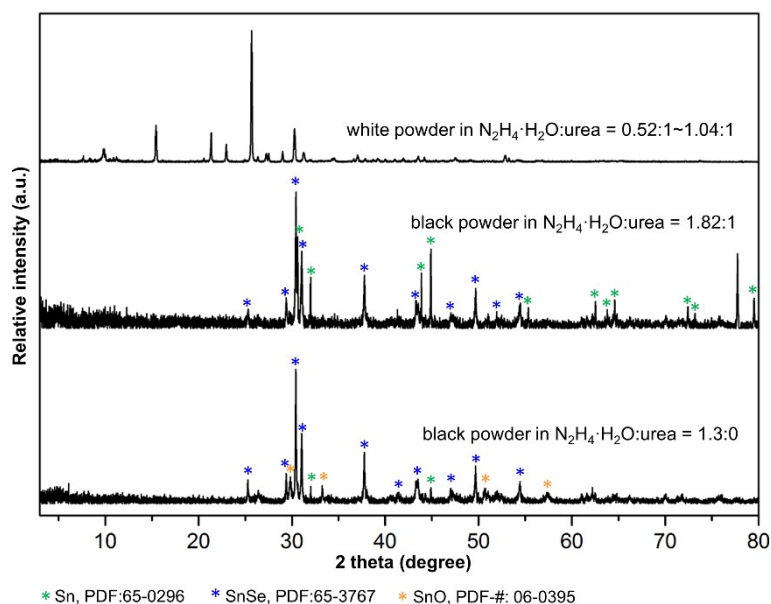


Figure S7. PXRD patterns for the by-products obtained from the reactions with different $\text{N}_2\text{H}_4\cdot\text{H}_2\text{O}:\text{urea}$ ratio at 150 °C.

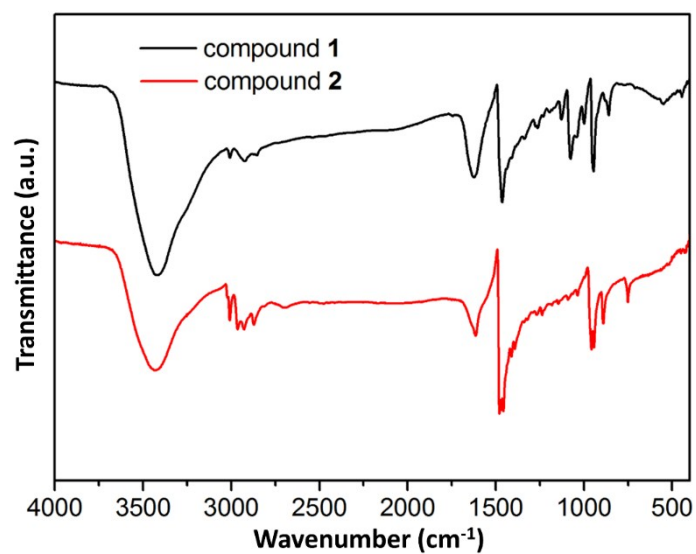


Figure S8. FTIR spectra of compound **1** and **2** measured at room temperature on KBr pellets.

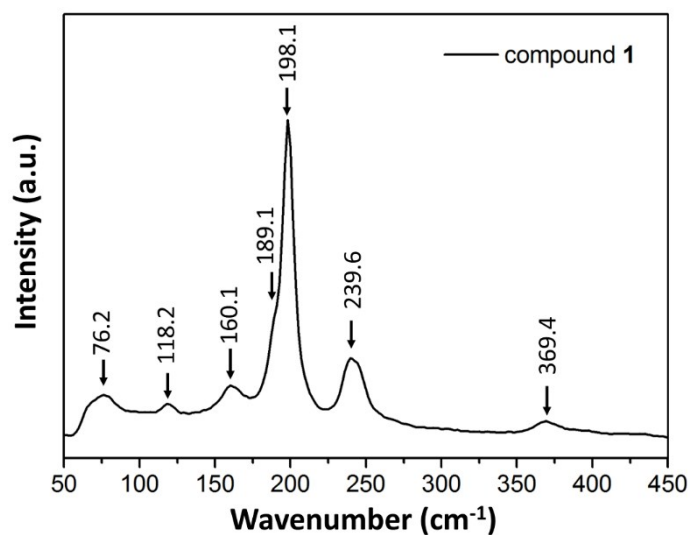


Figure S9. Single-crystal Raman spectrum of compound **1** measured at room temperature.

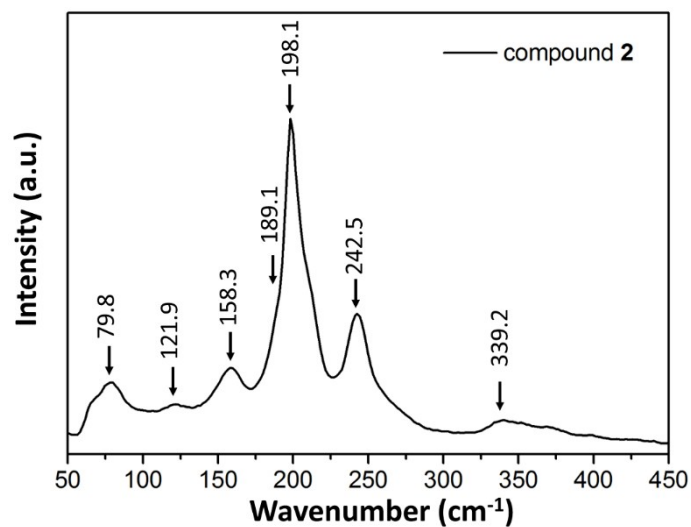
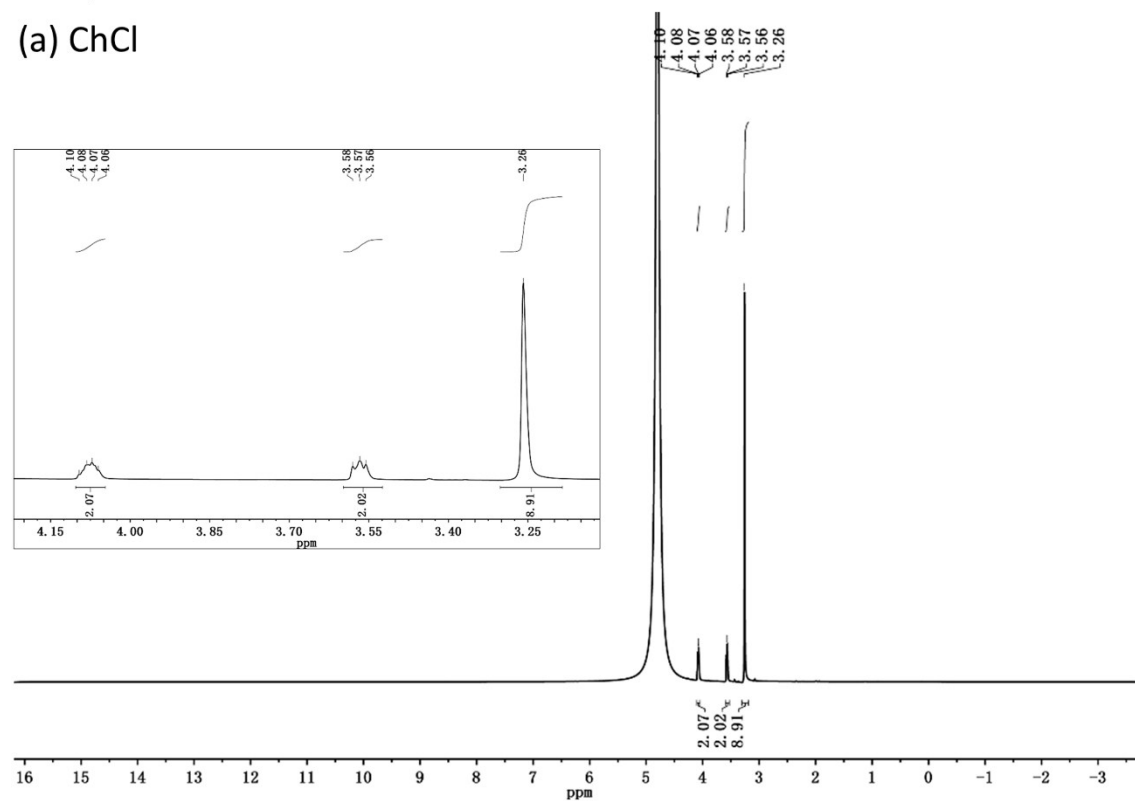


Figure S10. Single-crystal Raman spectrum of compound **2** measured at room temperature.

^1H spectra

(a) ChCl



(b) compound **1**

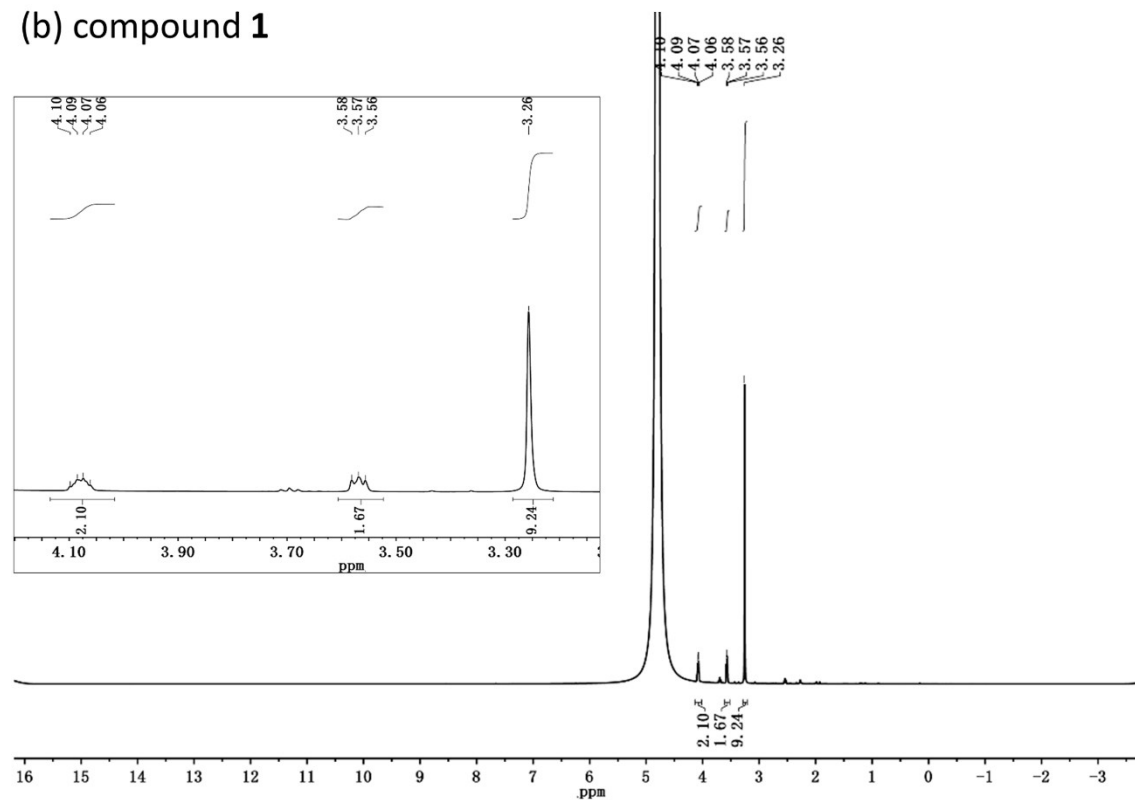
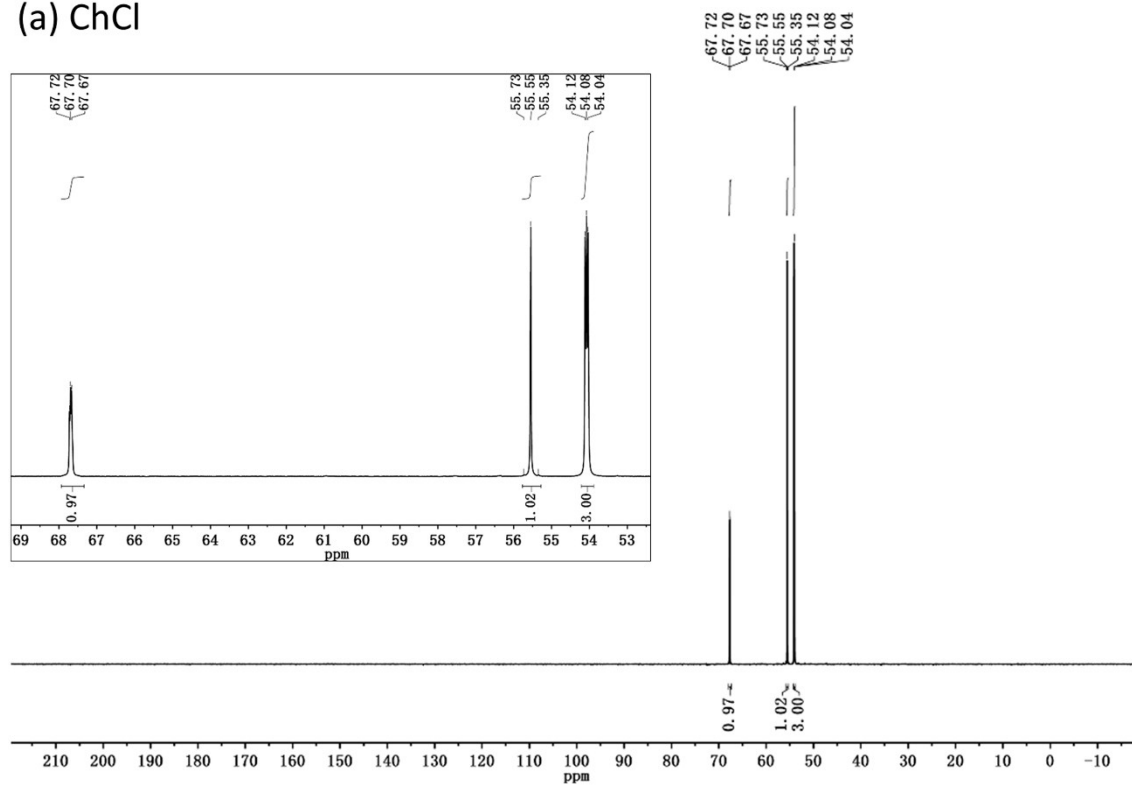


Figure S11. ^1H NMR spectra of (a) ChCl and (b) compound **1** dissolved in $\text{N}_2\text{H}_4\cdot\text{H}_2\text{O}$ (98%)/ D_2O recorded at room temperature.

^{13}C spectra

(a) CHCl_3



(b) compound 1

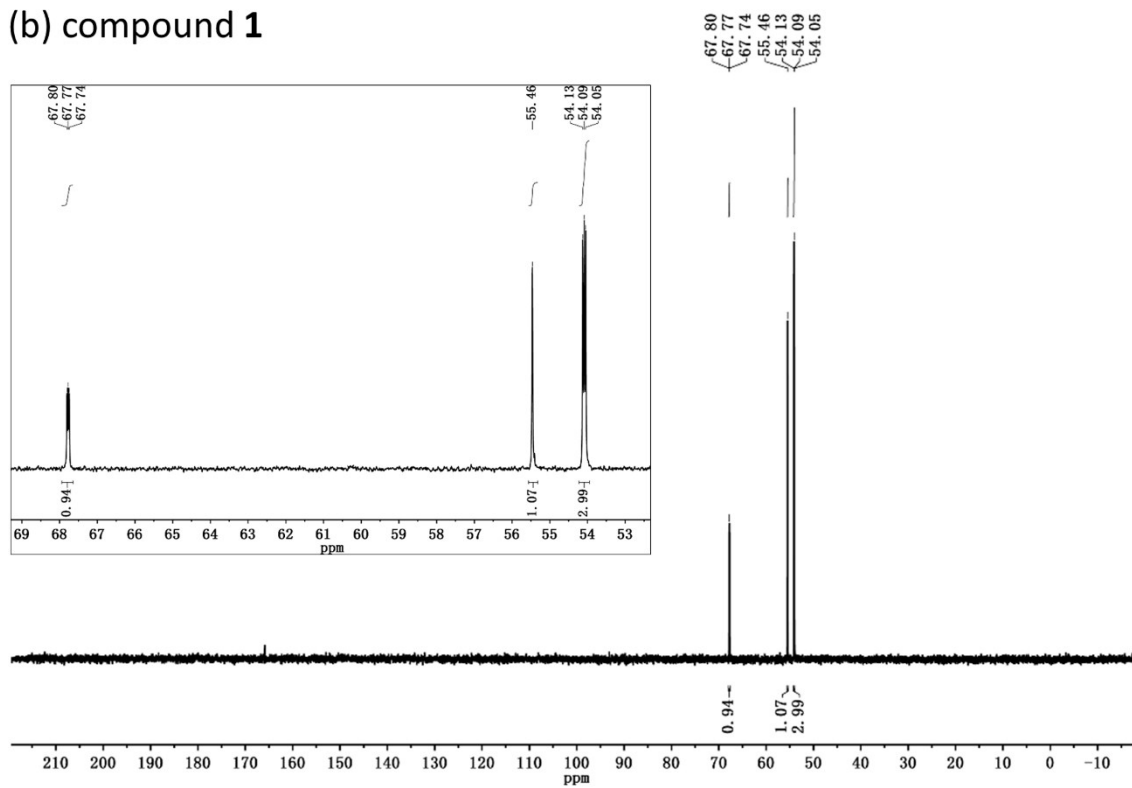
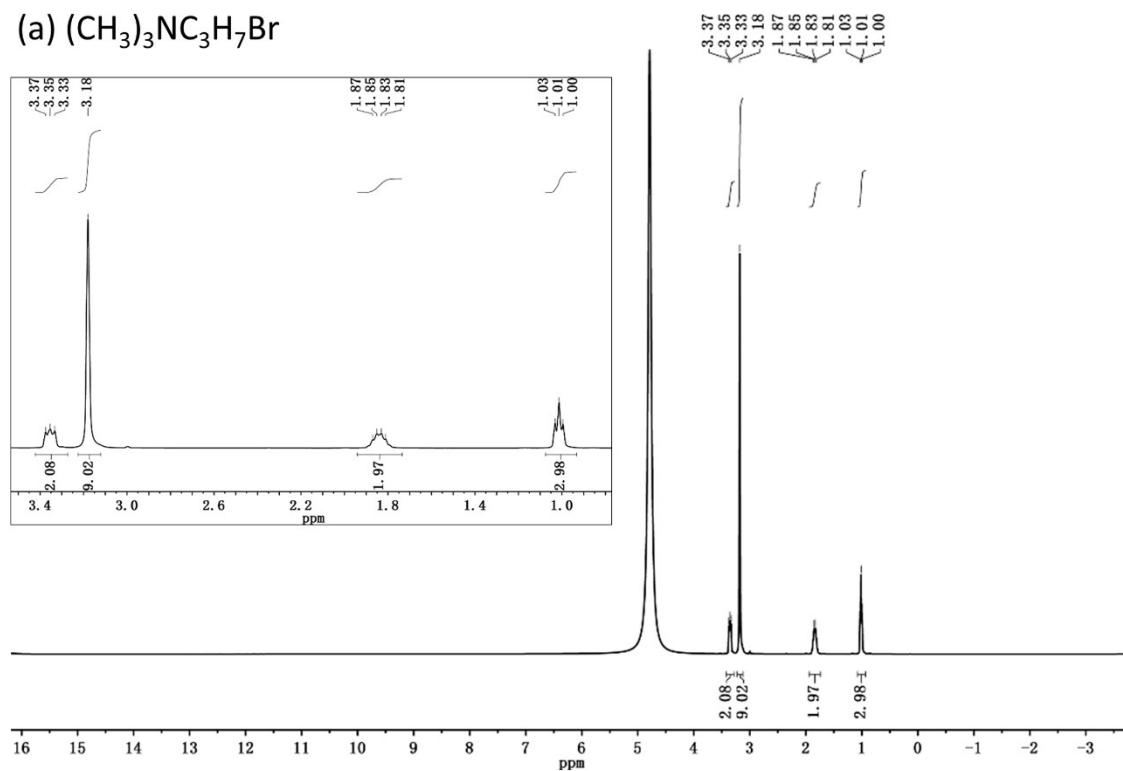


Figure S12. ^{13}C NMR spectra of (a) CHCl_3 and (b) compound 1 dissolved in $\text{N}_2\text{H}_4 \cdot \text{H}_2\text{O}$ (98%) / D_2O recorded at room temperature.

^1H spectra

(a) $(\text{CH}_3)_3\text{NC}_3\text{H}_7\text{Br}$



(b) compound 2

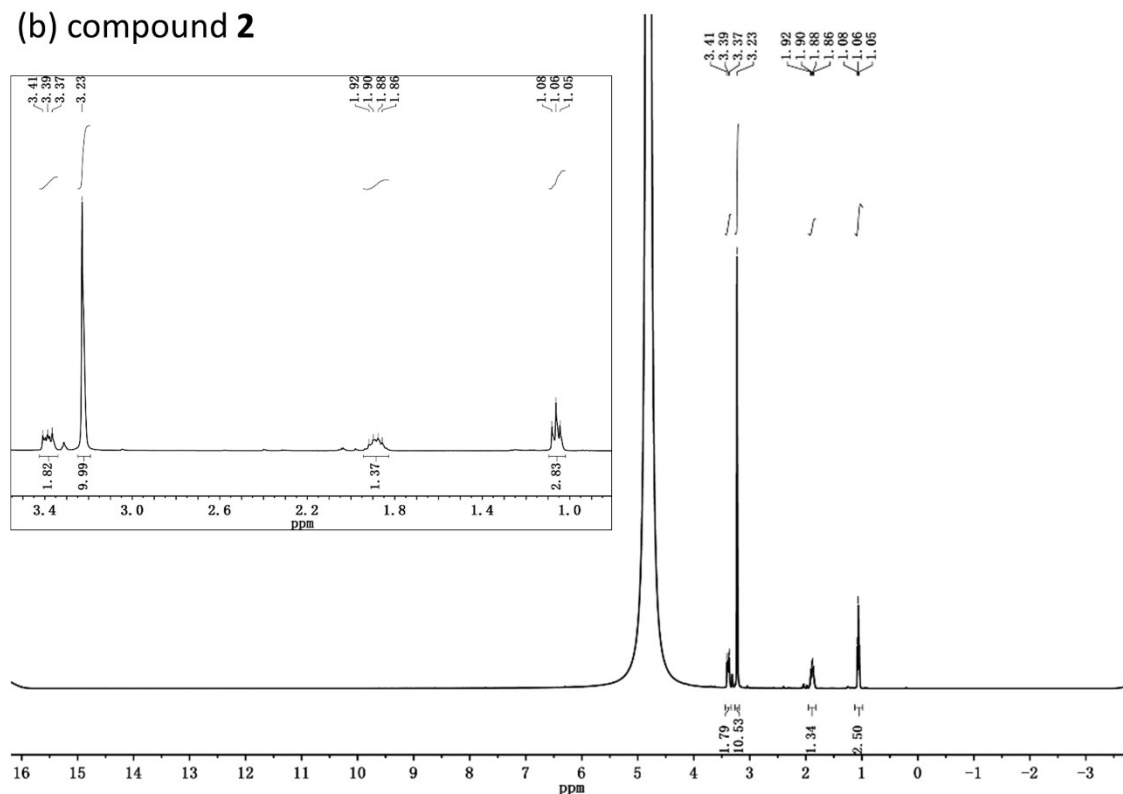
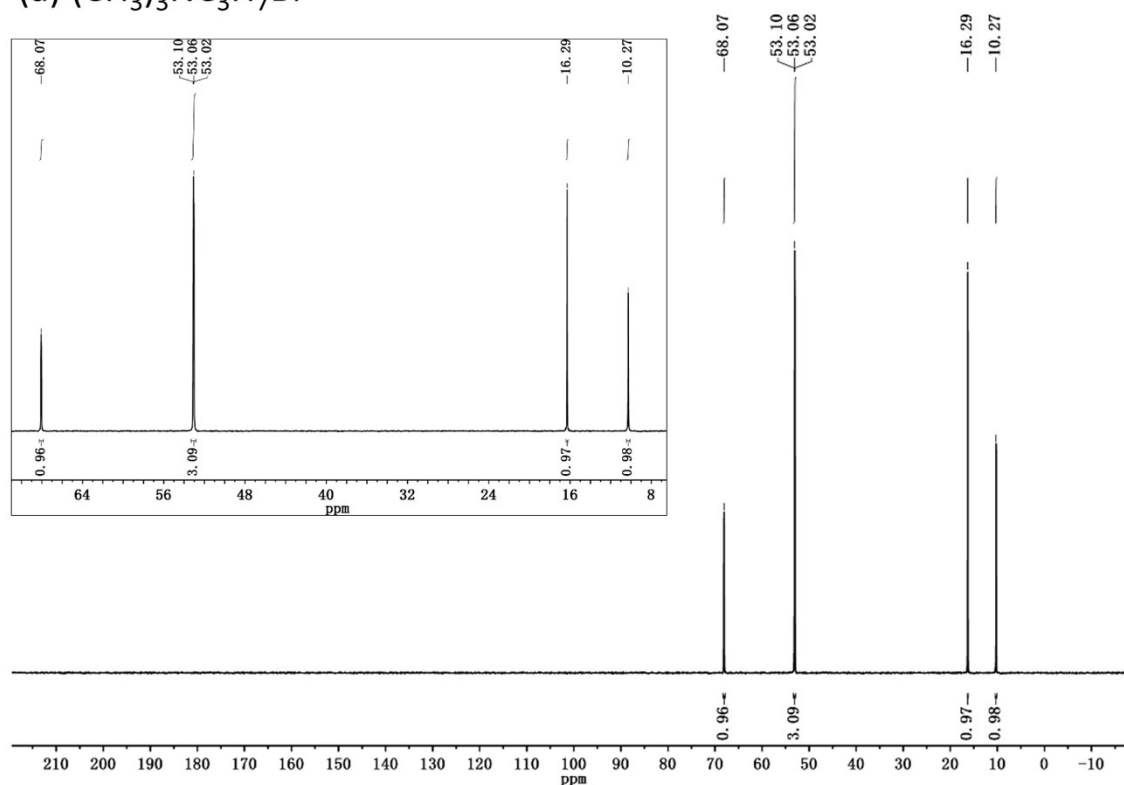


Figure S13. ^1H NMR spectra of (a) $(\text{CH}_3)_3\text{NC}_3\text{H}_7\text{Br}$ and (b) compound 2 dissolved in $\text{N}_2\text{H}_4 \cdot \text{H}_2\text{O}$ (98%)/ D_2O recorded at room temperature.

^{13}C spectra

(a) $(\text{CH}_3)_3\text{NC}_3\text{H}_7\text{Br}$



(b) compound 2

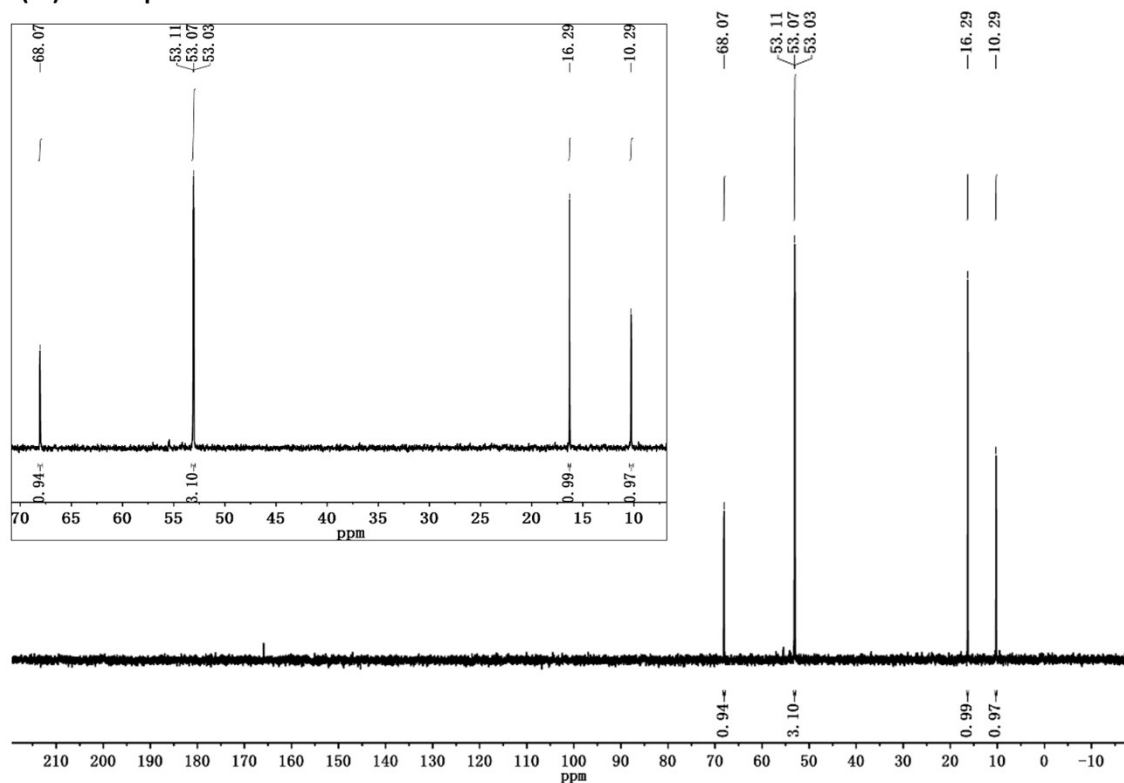


Figure S14. ^{13}C NMR spectra of (a) $(\text{CH}_3)_3\text{NC}_3\text{H}_7\text{Br}$ and (b) compound 2 dissolved in $\text{N}_2\text{H}_4 \cdot \text{H}_2\text{O}$ (98%)/ D_2O recorded at room temperature.

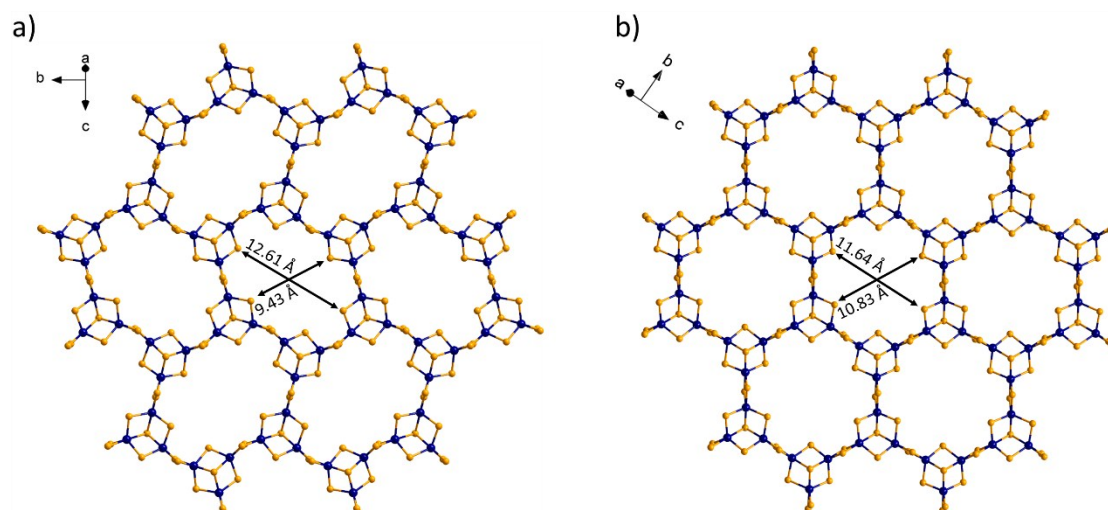


Figure S15. Comparison of the $[\text{Sn}_3\text{Se}_7]_n^{2n-}$ layers in compound **1** at (a) 100 K and 420 K. The window dimensions were obtained by measuring the corresponding Se...Se distance (excluding the van der Waals radii of Se atoms) using Diamond software (Version 3.2k, copyright Crystal Impact GbR).

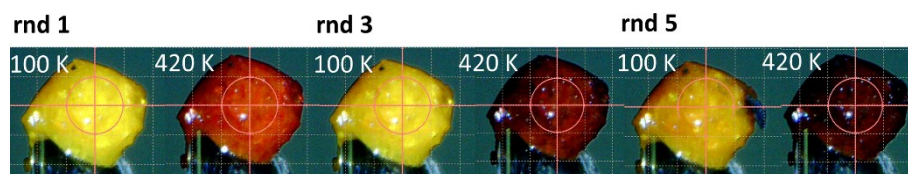


Figure S16. Colour change of the polycrystalline sample **1** at 100 K and 420 K in the five-round test.

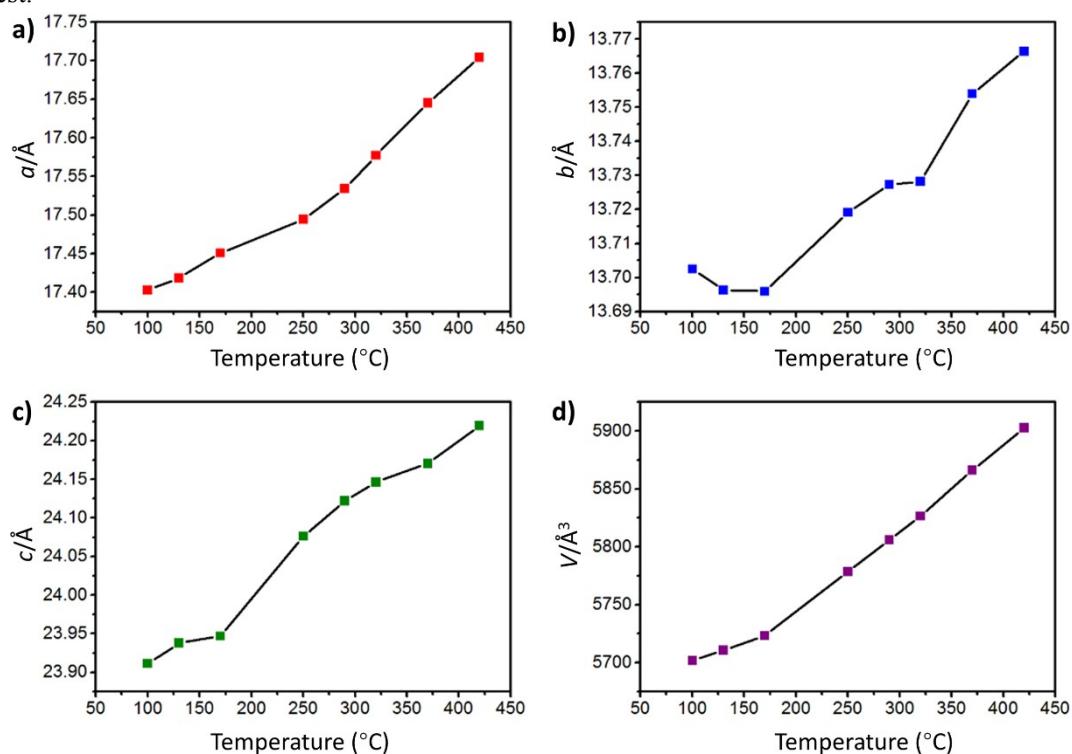


Figure S17. Variation of the unit cell parameters (a) a , (b) b , (c) c and (d) volume of compound **2** versus temperature. Data were obtained from the temperature-varied single crystal XRD measurement.

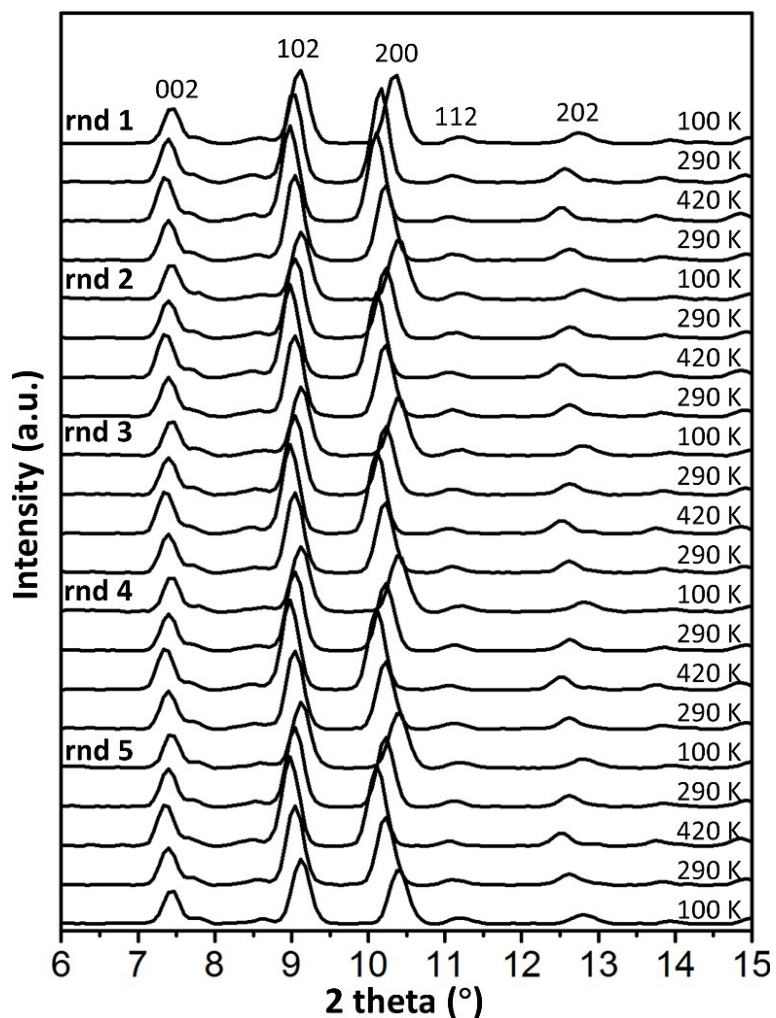


Figure S18. Five rounds of temperature-dependent PXRD patterns for compound **2** varying from 100 K to 420 K, and then back to 100 K. The identification of each round indicates an excellent thermal stability of the title compound.



Figure S19. Colour change of a single crystal of $(\text{TMA})_2\text{Sn}_3\text{Se}_7$ from 100 K to 290 K.

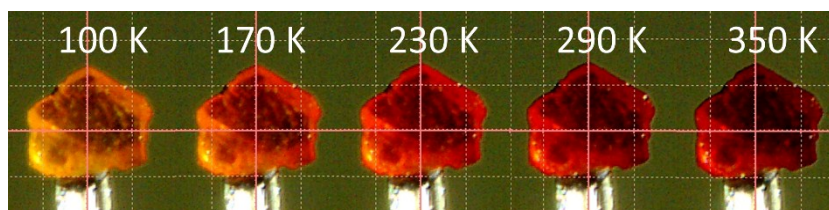


Figure S20. Colour change of a single crystal of $[\text{enH}_2][\text{Sn}_3\text{Se}_7] \cdot 0.5\text{en}$ from 100 K to 350 K.

References:

- [1] G. M. Sheldrick, A short history of SHELX, *Acta Crystallogr. Sect. A* 2008, 64, 112-122.
- [2] W. S. Sheldrick, H.-G. Braunbeck, Preparation and crystal structure of $\text{Cs}_2\text{Sn}_3\text{Se}_7$, a cesium selenostannate(IV) with pentacoordinated Tin, *Z. Naturforsch. B* 1990, 45, 1643-1646.
- [3] W. S. Sheldrick, H. G. Braunbeck, Preparation and crystal structure of ethylenediammonium selenostannates(IV) and $[\text{2SnSe}_2\cdot\text{en}]_x$, *Z. Anorg. Allg. Chem.* 1993, 619, 1300-1306.
- [4] H. Aizari, G. A. Ozin, R. L. Bedard, S. Petrov, D. Young, Synthesis and Compositional Tuning of the Band Properties of Isostructural TMA-SnS_xSe_{1-x}-1 Nanoporous Materials, *Adv. Mater.* 1995, 7, 370-374.
- [5] J. B. Parise, Y. Ko, K. Tan, D. M. Nellis, S. Koch, Structural evolution from tin sulfide (selenide) layered structures to novel 3- and 4-connected tin oxy-sulfides, *Solid State Chem.* 1995, 117, 219-228.
- [6] A. Fehlker, R. Blachnik, Synthesis, structure, and properties of some selenidostannates. II. $[(\text{C}_2\text{H}_5)_3\text{NH}]_2\text{Sn}_3\text{Se}_7\cdot 0.25\text{H}_2\text{O}$ und $[(\text{C}_3\text{H}_7)_2\text{NH}_2]_4\text{Sn}_4\text{Se}_{10}\cdot 4\text{H}_2\text{O}$, *Z. Anorg. Allg. Chem.* 2001, 627, 1128-1134.
- [7] S. Lu, Y. Ke, J. Li, S. Zhou, X. Wu, W. Du, Solvothermal synthesis and structure of two 2D tin-selenides with long alkyldiamine $\text{NH}_2(\text{CH}_2)_n\text{NH}_2$ ($n = 8, 10$), *Struc. Chem.* 2003, 14, 637-642.
- [8] G.-H. Xu, C. Wang, P. Guo, Poly[[[pentaethylenehexamine)manganese(II)] [hepta- μ -selenidotritin(IV)]]: a tin-selenium net with remarkable flexibility, *Acta Cryst. C* 2009, 65, m171-m173.
- [9] G.-N. Liu, G.-C. Guo, M.-J. Zhang, J.-S. Guo, H.-Y. Zeng, J.-S. Huang, Different effects of a cotemplate and [(transition-metal)(1,10-phenanthroline)_m]²⁺ ($m = 1-3$) complex cations on the self-assembly of a series of hybrid selenidostannates showing combined optical properties of organic and inorganic components, *Inorg. Chem.* 2011, 50, 9660-9669.
- [10] J.-R. Li, W.-W. Xiong, Z.-L. Xie, C.-F. Du, G.-D. Zou, X.-Y. Huang, From selenidostannates to silver-selenidostannate: structural variation of chalcogenidometallates synthesized in ionic liquids, *Chem. Comm.* 2013, 49, 181-183
- [11] W.-W. Xiong, J. Miao, K. Ye, Y. Wang, B. Liu, Q. Zhang, Threading chalcogenide layers with polymer chains, *Angew. Chem. Int. Ed.* 2015, 54, 546-550.
- [12] J. Lu, Y. Shen, F. Wang, C. Tang, Y. Zhang, D. Jia, Solvothermal syntheses and characterizations of selenidostannate salts of transition metal complex cations: conformational flexibility of the lamellar $[\text{Sn}_3\text{Se}_7]_n$ Anion, *Z. Anorg. Allg. Chem.* 2015, 641, 561-567.
- [13] S. Santner, S. Dehnen, $[\text{M}_4\text{Sn}_4\text{Se}_{17}]^{10-}$ cluster anions ($\text{M} = \text{Mn}, \text{Zn}, \text{Cd}$) in a Cs^+ environment and as ternary precursors for ionothermal treatment, *Inorg. Chem.* 2015, 54, 1188-1190.
- [14] C.-F. Du, J.-R. Li, M.-L. Feng, G.-D. Zou, N.-N. Shen, X.-Y. Huang, Varied forms of lamellar $[\text{Sn}_3\text{Se}_7]_n^{2n-}$ anion: the competitive and synergistic structure-directing effects of metal-amine complex and imidazolium cations, *Dalton Trans.* 2015, 44, 7364-7372.
- [15] D. D. Hu, Y. Y. Zhang, H. J. Yang, J. Lin, T. Wu, Structural transformation of selenidostannates from 1D to 0D and 2D via a stepwise amine-templated assembly strategy, *Dalton Trans.* 2017, 46, 7534-7539.